Validating Plate Boundary Observatory borehole strainmeter data with GNSS derived strain

Trever T. Hines and Eric A. Hetland

July 22, 2017

1 Introduction

The Plate Boundary Observatory (PBO) maintains 82 borehole strain meters (BSMs), most of which are installed along the Western United States. BSMs are able to detect geophysical processes such as coseismic and postseismic deformation (e.g., Langbein et al., 2006; Langbein, 2015), slow slip events (e.g., Dragert and Wang, 2011), and seismic wave propagation (Barbour and Crowell, 2017). BSMs are intended for measuring deformation over timescales of minutes to months. At longer timescales, BSM data is contaminated by factors such as borehole relaxation (Gladwin et al., 1987). Slow slip events and postseismic deformation occur on timescales that near the upper limit of what BSMs can be expected to resolve. Another complication with BSM data is that the strain measured at the borehole may deviate from the regional strain due to local topographic or geologic features (Berger and Beaumont, 1976). Due to these sources of noise, it can be difficult to use BSM data quantitatively in, for example, geophysical inverse problems. In this study, we assess the ability of BSMs to measure strain resulting from slow slip events (SSEs) on the Cascadia subduction zone. This is done by comparing BSM data to strain derived from GNSS data.

There are about forty BSMs in the Pacific Northwest and only five of them, B003, B004, B005, B007, and B018, record noticeable deformation from SSEs. Of these stations B005 and B007 are collocated. We show that only station B004 produces strain that is in reasonable agreement with GNSS derived strain rates. Station B018 records shear strains with opposite polarity as the GNSS derived strains. This discrepancy can be explained by an 25° error in the recorded orientation of the instrument.

GNSS derived strains are computed with Gaussian process regression using the method described in (Hines and Hetland, 2017b).

2 BSM Data

The are about forty PBO BSMs in the Pacific Northwest, and only five of them, B003, B004, B005, B007, and B018, record noticeable deformation from SSEs. We limit our attention to these five station in this study. The remaining stations either contain too much noise on the timescale of SSEs or are too far away from the SSEs to observe any strain. Each of the PBO BSMs are Gladwin four-component tensor strainmeters, which are about 2 m long, 8.7 cm in diameter, and are installed at about 100 to 200 m depth. Each BSM contains four extensometers, or gauges. Only three gauges are necessary to completely determine the horizontal strain tensor, and the fourth gauge is included for redundancy. Gauges 1, 2, and 3 are oriented 60°, 120°, and 150° counterclockwise from gauge 0.

We use the level 2 gauge data provided by UNAVCO at www.unavco.org, which has undergone several post-processing steps. In the level 2 gauge data a borehole curing trend is estimated and removed by fitting two exponential terms and a linear trend to the data. The level 2 data is corrected for tidal strains by estimating and removing sinusoids with known tidal frequencies. There is also a correction for barometric pressure because the normal stress imposed on the surface by barometric pressure results in horizontal strains recorded by the BSM. The barometric pressure correction is the observed barometric pressure at each site multiplied by a best fitting scaling factor. Lastly, offsets have been removed in the level 2 data product.

We denote the extension measured at gauge i as e_i, and the strain tensor components as ε_{xx}, ε_{yy}, and ε_{xy}, where x and y indicate the east and north direction, respectively. The extensions measured at BSMs are traditionally converted into areal strain, $\varepsilon_a = \varepsilon_{xx} + \varepsilon_{yy}$, differential strain $\varepsilon_d = \varepsilon_{xx} - \varepsilon_{yy}$, and engineering shear strain, $\varepsilon_s = 2\varepsilon_{xy}$. In this study, we will compare ε_a, ε_d, and ε_s recorded at the BSMs to those predicted by GNSS data. Using θ_0 to denote the orientation of gauge 0, in degrees north of east, these strain components can be expressed in terms of the gauge measurements through the equation

$$\left[\begin{array}{c}\varepsilon_a\\ \varepsilon_d\\ \varepsilon_s\end{array}\right] = 2\mathbf{K}^{-1}\left[\begin{array}{ccc}1 & \cos(2\theta_0) & \sin(2\theta_0)\\ 1 & \cos(2(\theta_0+60)) & \sin(2(\theta_0+60))\\ 1 & \cos(2(\theta_0+120)) & \sin(2(\theta_0+120))\\ 1 & \cos(2(\theta_0+150)) & \sin(2(\theta_0+150))\end{array}\right]^{+}\left[\begin{array}{c}e_0\\ e_1\\ e_2\\ e_3\end{array}\right], \tag{1}$$

where "+" indicates the Moore-Penrose pseudoinverse and $\mathbf{K}$ is a coupling matrix describing how the instrument strains relate to the crustal strains (Hart et al., 1996). In this paper ε_a, ε_d, and ε_s are ideally intended to represent crustal strains. We assume that BSMs are installed in homogeneous, isotropic rock, allowing us to write the coupling matrix as

$$\mathbf{K} = \left[\begin{array}{ccc}c & 0 & 0\\ 0 & d & 0\\ 0 & 0 & d\end{array}\right], \tag{2}$$

where c, and d are response factors that depend on the elastic properties of the instrument, the grout, and surrounding rock (Gladwin and Hart, 1985). Based on the analysis of Gladwin and Hart (1985), we use $c = 1.5$ and $d = 3.0$. UNAVCO, the organization responsible for maintaining the PBO BSMs and disseminating their data, use these same response factors for their final data products.

Local topographic or geologic features can cause $\mathbf{K}$ to have non-zero off diagonal elements. If possible, the components of $\mathbf{K}$ should be determined in-situ by calibrating the BSM data with a well known strain source, such as diurnal and semi-diurnal tides (Hart et al., 1996; Roeloffs, 2010; Hodgkinson et al., 2013). Hart et al. (1996) calibrated a BSM at Pinyon Flat, using the tidal strains recorded at a collocated laser strain meter. This calibration method is, of course, not possible for most PBO BSMs. Roeloffs (2010) and Hodgkinson et al. (2013) calibrated PBO BSMs using theoretical predictions of tidal strains (e.g., Agnew, 1997). This approach is still not adequate for BSMs near large local bodies of water, which can make it difficult to form an accurate theoretical estimate of tidal strains. As determined by Roeloffs (2010), the five BSM stations considered in this paper are too close to the Straight of Juan de Fuca to be accurately calibrated with tidal strains. Since in-situ calibration is not possible, we acknowledge that our choice for $\mathbf{K}$ is likely to be a significant source of error in BSM data. Another potential source of error is the assumed orientation for θ_0. This orientation is determined by a compass on the instrument, and it is possible that magnetic minerals in the surrounding rock can give the compass an erroneous reading.

3 GNSS derived strain

We compare the BSM strain components to transient strains estimated from GNSS data. In this paper, transient strain is considered to be any deviation from the steady rate of strain accumulation from plate tectonics. We use daily GNSS displacement solutions for 94 continuous GNSS stations in the Pacific Northwest (Figure 1). The data is available from www.unavco.org. We convert the GNSS data to transient strains using Gaussian process regression (GPR) as described in Hines and Hetland (2017a). With GPR, we select a prior spatio-temporal covariance model for the geophysical signal that we want to recover. Following Hines and Hetland (2017a), we assume that our prior for displacements is a Gaussian process with zero mean, and covariance function described by

$$C_u((t,x),(t',x')) = \phi^2 T(t,t') X(x,x'), \tag{3}$$

where T is the Wendland covariance function

$$T(t,t') = \left(1 - \frac{|t-t'|}{\tau}\right)_+^5 \left(\frac{8|t-t'|^2}{\tau^2} + \frac{5|t-t'|}{\tau} + 1\right), \tag{4}$$

and X is the squared exponential covariance function

$$X(\vec{x},\vec{x}') = \exp\left(\frac{-||\vec{x}-\vec{x}'||_2^2}{2\ell^2}\right). \tag{5}$$

The hyperparameters ϕ, τ, and ℓ control the amplitude, characteristic time-scale, and characteristic length-scale of the prior. Hines and Hetland (2017a) found that the optimal hyperparameters for describing displacements from SSEs are roughly $\phi = 0.5$ mm, $\tau = 0.1$ yr, and $\ell = 100$ km. These parameters were chosen objectively using maximum likelihood methods; however based on our experience, this prior may not be sufficiently flexible to described all the observed data. Consequently, we explore using lower values for τ and ℓ and a higher value for ϕ. For each tested set of hyperparameters, we condition the prior with the observed GNSS data and visually compare the posterior displacements to the observations. We settle on the values $\phi = 1.0$ mm, $\tau = 0.05$ yr, and $\ell = 80$ km. With this final set of hyperparameters, we condition the prior with the GNSS data and then spatially differentiate the posterior displacements to obtain transient strain.

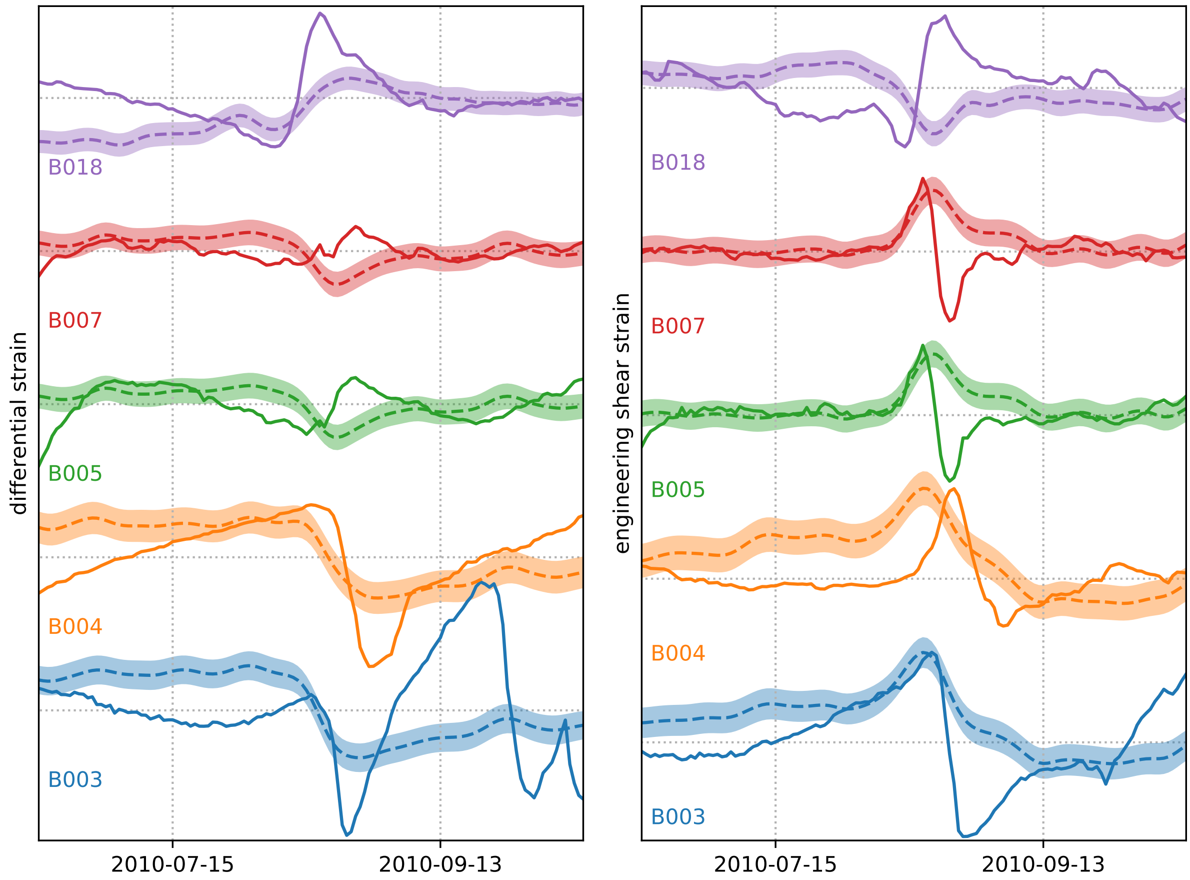

Figure 1: foo

4 Results

5 Reorienting B018

References

Agnew, D. C. (1997). NLOADF: A program for computing ocean-tide loading. *Journal of Geophysical Research*, 102:5109–5110.

Barbour, A. J. and Crowell, B. W. (2017). Dynamic Strains for Earthquake Source Characterization. *Seismological Research Letters*, 88(2A):354–370.

Berger, J. and Beaumont, C. (1976). An analysis of tidal strain observations from the United States of America II. The inhomogeneous tide. *Bulletin of the Seismological Society of America*, 66(6):1821–1846.

Dragert, H. and Wang, K. (2011). Temporal evolution of an episodic tremor and slip event along the northern Cascadia margin. *Journal of Geophysical Research: Solid Earth*, 116(12):1–12.

Gladwin, M. T., Gwyther, R. L., Hart, R., Francis, M., and Johnston, M. J. S. (1987). Borehole tensor strain measurements in California. *Journal of Geophysical Research: Solid Earth*, 92(B8):7981–7988.

Gladwin, M. T. and Hart, R. (1985). Design parameters for borehole strain instrumentation. *Pure and Applied Geophysics*, 123(1):59–80.

Hart, R. H. G., Gladwin, M. T., Gwyther, R. L., Agnew, D. C., and Wyatt, F. K. (1996). Tidal calibration of borehole strain meters: Removing the effects of small-scale inhomogeneity. *Journal of Geophysical Research*, 101(96).

Hines, T. T. and Hetland, E. A. (2017a). Revealing transient strain in geodetic data with Gaussian process regression. *submitted to Geophysical Journal International*, pages 1–25.

Hines, T. T. and Hetland, E. A. (2017b). Unbiased characterization of noise in geodetic data. *submitted to Journal of Geodesy.*

Hodgkinson, K., Agnew, D., and Roeloffs, E. (2013). Working With Strainmeter Data. *Eos, Transactions American Geophysical Union*, 94(9):91–91.

Langbein, J. (2015). Borehole strainmeter measurements spanning the 2014 Mw6.0 South Napa Earthquake, California: The effect from instrument calibration. *Journal of Geophysical Research B: Solid Earth*, 120(10):7190–7202.

Langbein, J., Murray, J. R., and Snyder, H. A. (2006). Coseismic and initial postseismic deformation from the 2004 Parkfield, California, earthquake, observed by global positioning system, electronic distance meter, creepmeters, and borehole strainmeters. *Bulletin of the Seismological Society of America*, 96(4 B):304–320.

Roeloffs, E. (2010). Tidal calibration of Plate Boundary Observatory borehole strainmeters: Roles of vertical and shear coupling. *Journal of Geophysical Research: Solid Earth*, 115(6):1–25.